Separation and Purification Technology 363 (2025) 132200

Contents lists available at ScienceDirect

Separation and Purification Technology

journal homepage: www.elsevier.com/locate/seppur

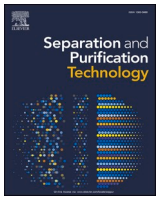

Efficient extraction and purification of mycosporines-like amino acids (MAAs) following a multiproduct biorefinery approach

Bárbara M.C. Vaz [a,1], Maria Sofia C.T.S. Leite [a,1], Letícia S. Contieri [a,b], Leonardo M. de Souza Mesquita [a,b], Alexandra Conde [a], Joana P. Oliveira [a], Diana C.G.A. Pinto [c], Sónia P.M. Ventura [a,*]

[a] CICECO – Aveiro Institute of Materials, Department of Chemistry, University of Aveiro, Campus Universitário de Santiago, 3810-193 Aveiro, Portugal
[b] Multidisciplinary Laboratory of Food and Health (LabMAS), School of Applied Sciences (FCA), University of Campinas, Rua Pedro Zaccaria 1300, 13484-350, Limeira, São Paulo, Brazil
[c] LAQV - REQUIMTE, Department of Chemistry, University of Aveiro, 3810-193 Aveiro, Portugal

ARTICLE INFO

Keywords:
Red Macroalgae
Gracilaria sp.
Solid-liquid extraction
Ultrafiltration
Induced Precipitation
Mycosporine-like amino acids

ABSTRACT

A marine bio-based economy has emerged as a sustainable and renewable solution to address the resource depletion of fossil fuels and ensure a responsible and sustainable utilization of natural resources by following a multi-product biorefinery approach. Macroalgae are a valuable source of several high-demand compounds including mycosporine-like amino acids (MAAs), which can absorb UV radiation and protect the skin from external damage. In this work, a sustainable and multi-product biorefinery was designed from *Gracilaria* sp. by applying a solid–liquid extraction followed by two purification steps, ultrafiltration and induced precipitation. This process enabled the recovery of three valuable compound fractions, one rich in phycobiliproteins, a second, rich in non-fluorescent proteins, and a third, rich in MAAs (main goal), specifically porphyra-334. In addition, by 2,2′-azino-bis(3-ethylbenzothiazoline-6-sulfonic acid) (ABTS) scavenging assay, MAAs-rich fraction revealed enhanced antioxidant activity. Lastly, a comprehensive conceptual design of the process was created, envisioning its implementation at an industrial scale.

1. Introduction

The responsible and sustainable exploitation of natural resources is crucial to the planet's survival [1]. Resources like water, minerals, energy, and land are in greater demand as industrialization and world population growth continue. This burdens ecosystems heavily and may result in biodiversity loss, climate change, and environmental deterioration [2]. Governments, organizations, and individuals are starting to adopt sustainable practices and supporting the shift to renewable and regenerative resources due to recognizing the importance of implementing a green economy [3]. As an example, the company L'Oréal set a sustainable commitment to preserve the resource limitations of our planet following the guidelines of the 2030 Agenda for Sustainable Development. Until 2030, they intend to improve the energy efficiency of their production pipelines and use 100% renewable energy, recycle, and reuse 100% of the used water in a loop to respect the aquatic ecosystems. Moreover, they will focus on replacing 100% of their ingredients with bio-based compounds derived from renewable natural resources and, finally, ensure circular alternatives for packaging, recycling, waste management, logistics, and eco-efficient processes by promoting a circular economy [4].

Algae biomass presents a promising solution for acquiring natural resources as a renewable and sustainable feedstock. With only resources like water, sunlight, and CO_2, algae can grow without competing with conventional crops. Nutrients for their growth can be easily acquired from household or industrial wastewater, and algae can efficiently assimilate CO_2 [5]. In addition to their cultivation advantages compared to other renewable feedstocks, algae are a rich source of various high-value compounds with high market value, including pigments, lipids, proteins, and carbohydrates, among others [6]. Cosmetics, pharmaceuticals, and nutraceuticals are some industries where these compounds can be applied, with great promise as the future of natural

* Corresponding author.
E-mail address: spventura@ua.pt (S.P.M. Ventura).
[1] Both authors worked equally for this manuscript.

https://doi.org/10.1016/j.seppur.2025.132200
Received 14 January 2025; Accepted 20 February 2025
Available online 25 February 2025

ingredients [7]. However, the industrial utilization of algae feedstocks is still not economically feasible because of their costs, energy needs, and limited availability of biomass and biomolecules [8]. By converting biomass into biofuels and high-value products, the biorefinery approach offers the potential to maximize the value of raw materials. This approach aims to minimize or eliminate waste generation by utilizing all biomass potential to produce multiple profitable products, ultimately, enabling the reduction of environmental impacts while enhancing the economic viability of the process [9].

Red seaweed species contribute 61% to global seaweed production, an excellent raw material for biorefineries [10]. Mycosporine-like amino acids (MAAs) stand out among the biocompounds in this class largely because of their photoprotection [11], antioxidant properties [12], and excellent photo- and thermo-stability [13], which are desirable qualities for the creation of cosmetic products [14]. They are characterized by their small size and water solubility, consisting of either an aminocyclohexenone or an aminocycloheximine ring, with nitrogen or amino alcohol substituents. Marine organisms produce MAAs in response to intense UV stress, giving them the ability to serve as effective UV shields by absorbing and dissipating UV radiation as harmless heat, thereby preventing reactive oxygen species (ROS) production, oxidative stress, and DNA damage [15].

While the current world market offers a plethora of UV-protective compounds, it is worth noting that 98% of them primarily protect the UV-B range. The remaining 2% demonstrate effectiveness against only the far UV-A range [16]. This is where MAAs stand out as the most potent natural compounds for absorbing UV-A radiation [17]. Hence, there is a critical demand for sunscreen agents offering broad-spectrum protection against the harmful UV range. A few commercial products have already been developed to substitute synthetic filters. An exemplary product, Helioguard® 365 based on mycosporine-like amino acids, has been demonstrated to effectively reduce lipid peroxidation and skin aging parameters, comparable to a formulation containing synthetic filters [18]. Nevertheless, the commercial utilization of MAAs has been hindered by costly and time-consuming cultivation and harvesting methods, challenging isolation processes, inconsistent MAA content, and environmental considerations [19].

Conventional extraction methods for MAAs involve using organic solvents like methanol, ethanol, or mixtures of methanol and ethanol with water, prolonged extraction times, high temperatures, and multiple process steps, which hinder their industrialization [12,20–23]. Moreover, they pose environmental concerns due to the use of organic solvents. Hence, developing simple and sustainable downstream processes with a multiproduct biorefinery approach is crucial to overcome the current difficulties and meeting the current market demands.

By recognizing MAAs as valuable compounds and the sustainable nature of algae biomass, this study aims to devise an efficient and sustainable method for extracting and purifying MAAs from *Gracilaria* sp. Adopting a biorefinery approach, the developed process intends to recover three valuable hydrophilic fractions, such as MAAs, phycobiliproteins, and non-fluorescent proteins.

2. Experimental section

2.1. Biomass

Fresh *Gracilaria* sp. was obtained from the company ALGAplus Lda based in Ílhavo (Portugal) between February and September 2022. ALGAplus produces marine algae in Ria de Aveiro (coast of Portugal) under an Integrated Multi-Trophic Aquaculture (IMTA) system and the rules of organic aquaculture of the European Union (EU). After collection, the macroalgae samples were washed several times with distilled water, frozen with liquid nitrogen, and grounded in a coffee grinder to disrupt the cell wall, standardizing the particle size, and improving the extraction process. In the end, the powder was frozen at −20 °C until further use.

2.2. Chemicals

Ammonium sulfate ($(NH_4)_2SO_4$, 99.5 wt%, CAS 7783-20-2) was purchased at Merck. Poly(acrylic acid) sodium salt with an average molecular weight of 8000 $g.mol^{-1}$ (NaPA 8000, 45 wt% in aqueous solution) and sodium phosphate dibasic heptahydrate ($Na_2HPO_4{\cdot}7H_2O$, 98–102 wt%, 7782-85-6) were acquired from Sigma-Aldrich. Ethanol (HPLC grade, CAS 64-17-5) and acetone (HPLC grade, CAS 67-64-1) were supplied by Fisher Scientific. Sodium chloride (NaCl, extra pure, CAS 7647-14-5), potassium chloride (KCl, 99.5 wt%, CAS 7447-40-7), and sodium phosphate dibasic anhydrous (Na_2HPO_4, 99 wt%, CAS 7558-79-4) were obtained from LabKem, Chem-Lab, and Fluka, respectively. Potassium phosphate monobasic (KH_2PO_4, pure, CAS 7778-77-0) was obtained from Honeywell. Citric acid ($C_6H_8O_7$, 99.5 wt %, CAS 77-92-9) and sodium phosphate monobasic (NaH_2PO_4, 99–100.5 wt%, CAS 7558-80-7) were supplied by Panreac. Sodium hydroxide (NaOH, 98 wt%, CAS 1310-73-2) was purchased at Fisher Scientific. Ultrapure water was obtained by double distillation, passed by a reverse osmosis system, and then treated with a Milli-Q plus 185 water purification apparatus.

2.3. Solid-liquid extraction

The solid–liquid extraction (SLE) process was initially performed following Martins *et al.* (2021) [24]. At first, 20 g of the previously pretreated fresh biomass was weighed, and 40 mL of distilled water was added, representing a solid–liquid ratio (SLR) of 0.5 $g_{fresh\ biomass}{\cdot}mL_{solvent}^{-1}$. SLE was performed in an orbital shaker (IKA KS 4000 ic control) for 20 min at room temperature (20 – 25 °C) and 250 rpm, protected from light exposure. After centrifugation of the samples in a Thermo Scientific Heraeus Megafuge 16R centrifuge at 4700 *g* for 30 min at 4 °C, the pellet was discarded, and the supernatant was kept. Next, other water-based solvents were tested and compared with distilled water using the same operating conditions, namely McIlvaine (0.1 M, pH 7), phosphate saline (1X, pH 7.4), and sodium phosphate (0.1 M, pH 7) buffers.

2.4. Optimization of solid–liquid extraction

A central composite rotatable design (CCRD – 2^2) was carried out in which the solid–liquid ratio (SLR, $g_{fresh\ biomass}{\cdot}mL_{solvent}^{-1}$) with a fixed volume of 10 mL, and the extraction time (t, min) were the two independent variables studied. In total, 11 assays were performed, 3 for the central point, 4 for the factorial points, and 4 for the axial points (see Table S1 in ESI to check the real and encoded values). Their performance was evaluated in terms of MAAs extraction yield ($mg_{MAAs}{\cdot}g_{fresh\ biomass}^{-1}$) and statistically analyzed with the software Statistica® 7 and a confidence level of 95%, following Dean *et al.* (1999) [25] and Rodrigues and Lemma (2014) [26] theory. Lastly, the optimum conditions found were validated in triplicate by calculating the means of relative deviation (%).

2.5. Ultrafiltration

Ultrafiltration was tested to maximize the purity of the MAAs obtained after the SLE step (procedure adopted by Martins *et al.* (2021) [24]), using two different centrifugal filter units, an Amicon ® Ultra – 0.5 mL Centrifugal Filter Unit of 3 kDa and other of 100 kDa, both from Merck Millipore. Briefly, 500 μL of the extract was added to each centrifugal filter unit and centrifuged at 14,000 *g* for 15 min to collect the permeate. Then, the filter was placed upside down for 2 min at 1000 *g* to collect the retentate, and 500 μL of ultrapure water was added to the retentate.

2.6. Induced precipitation

First, various protein precipitation procedures were tested using

ethanol, acetone, ammonium sulfate, and NaPA 8000. The ethanol and acetone precipitation procedure was based on Thermo Scientific [27]. Briefly, 1 mL of extract (obtained after ultrafiltration) was added to 4 mL of acetone/ethanol. Then, the samples were homogenized, put in the freezer at −20 °C overnight, and centrifuged (Thermo Scientific Heraeus Megafuge 16R) for 30 min at 14,000 *g*. The procedure for precipitation with ammonium sulfate and NaPA 8000 (45 wt%) was adapted from Martins *et al.* (2021) [24]. 0.4 g of ammonium sulfate/NaPA 8000 was mixed with the prepared extract until 2 g of total weight. The solutions were homogenized, left for 4 h at 4 °C, and then centrifuged under the same conditions described for ethanol/acetone. After separating all supernatants from the respective pellets, the samples were analyzed.

Then, aiming to induce the MAAs precipitation, the permeate pH (previously recovered) was varied between 11 and 12, adding, drop-by-drop, 2 M NaOH to make the solutions basic. After pH measurements, done in Metrohm 827 equipment, the solutions were homogenized and placed at 4 °C overnight as done in literature [24]. After that, the systems were centrifuged at 13,000 *g* for 5 min and the supernatant was analyzed. Finally, 500 μL of the precipitate was redissolved in PBS (1X, pH 7.4) to perform Folin-Ciocalteu and ABTS scavenging assays.

2.7. Compounds quantification

The UV–Visible spectra of all samples were measured between 200 and 700 nm in a UV–Vis microplate reader (Synergy HT-BioTek microplate reader). Total protein quantification (non-fluorescent proteins) was made using a previous calibration curve obtained for 280 nm (R^2 = 0.9976). For phycobiliproteins quantification (fluorescent proteins), R-phycoerythrin was used as standard at 565 nm (R^2 = 0.9998) since it was the most abundant phycobiliprotein found in *Gracilaria* sp. [28]. For MAAs, a porphyra 334 standard, obtained by us, was used and a calibration curve for 333 nm was prepared (R^2 = 0.9998). The standard obtention involved a solid–liquid extraction with water, followed by an additional ultrafiltration step utilizing a 100 kDa filter to eliminate fluorescent proteins. Subsequently, the content of non-fluorescent proteins was measured, and its impact was systematically excluded from the ensuing calculations. The yield of extraction for all the compounds was determined using Equation (1).

$$\text{Yield of extraction}\left(\text{mg}_{\text{compound}}\cdot\text{g}_{\text{fresh biomass}}{}^{-1}\right) = \frac{\text{Compound concentration}\,(\text{mg.mL}^{-1}) \times \text{Solvent volume}\,(\text{mL})}{\text{Weight of fresh biomass}\,(\text{g})} \quad (1)$$

To calculate the compound's recovery in the various purification steps, the mass of the compound in each fraction recovered was compared to the mass of the compound present in beginning of the respective step, Equation (2).

$$\text{Compound's recovery}\,(\%) = \frac{\text{Compound present in the recovered fraction}\,(\text{mg})}{\text{Compound present in beginning of the each step}\,(\text{mg})} \times 100 \quad (2)$$

2.8. High-performance liquid chromatography analysis (UHPLC-DAD-ESI/MS)

The initial extract was analyzed by UHPLC Ultimate 3000 (Dionex Co., San Jose, CA, USA), coupled to a UV detector (Dionex Co., San Jose, CA, USA) and a mass spectrometer (Thermo Scientific, San Jose, CA, USA) equipped with an electrospray ionization (ESI) interface. The elution was done with a mixture of 0.1% (v/v) of formic acid in water (A) and acetonitrile (B). The column system was Hypersil Gold (Thermo Scientific, USA) C_{18} (100 mm length; 2.1 mm i.d.; 1.9 μm particle diameter, capped). The default flow was kept at 0.2 mL.min^{-1}. The injection volume was 10 μL. UV–Vis spectral data were recorded in the 200 to 700 nm range, while chromatograms were recorded at 333 nm. The instrument was operated in negative-ion mode with an ESI needle voltage set at 5 kV and an ESI capital temperature of 275 °C. The full scan covered the *m/z* mass range between 100 and 2000. Nitrogen (purity > 99%) was used with a gas pressure set at 520 kPa (75 psi). CID-MS/MS and MS^2 experiments were simultaneously acquired for precursor ions using helium as the collision gas and with a collision energy of 25 to 35 arbitrary units. Compounds were identified by comparing MS and MS/MS spectra with those reported in the literature.

2.9. Folin-Ciocalteu (total phenolic content)

To determine the total phenolic content (TPC), the Folin–Ciocalteu colorimetric method was employed in a 96-well microplate, following a modified version of the method described by Coscueta *et al.* (2018) [29]. In this procedure, 30 μL of each sample was mixed with 100 μL of Folin-Ciocalteu reagent (20% v/v), followed by the addition of 100 μL of anhydrous sodium carbonate solution (7.4% m/v), adhering to the specified sequence. The resulting blue mixtures were thoroughly shaken and then incubated for 30 min at 25 °C. Subsequently, the absorbance of the mixtures was measured at 765 nm using a UV–Vis microplate reader (Synergy HT-BioTek microplate reader). To express the results as milligrams of gallic acid equivalents *per* milliliter of the sample ($mg_{GAE}.mL^{-1}$), a calibration curve of gallic acid (0.025–0.200 mg.mL^{-1}) was prepared, and the regression equation between absorbance and gallic acid concentration was calculated for each assay. The TPC values are reported as gallic acid equivalents (GAE), based on the calculated standard curve, with the results being expressed in $mg_{GAE}.mL^{-1}$ of the sample.

2.10. Antioxidant activity − ABTS scavenging assay

The ABTS scavenging assay was conducted in a 96-well microplate, following a modified version of the method described by Gonçalves *et al.* (2009) [30]. In this procedure, 20 μL of the sample, Trolox, or PBS (1X, pH 7.4) were combined with 180 μL of $ABTS^{\bullet+}$ working solution. The mixture was incubated for 5 min at 30 °C, and the absorbance at 734 nm was measured using a UV–Vis microplate reader (Synergy HT-BioTek microplate reader). The scavenging activity was expressed as the percentage reduction in absorbance compared to the control. The formula employed to calculate the percentage of scavenging is Equation (3).

$$\text{ABTS scavenging}\,(\%) = (A_{CTL} - A_{SPL}) * \frac{100}{A_{CTL}} \quad (3)$$

The regression equations correlating net ABTS scavenging with Trolox concentration were determined. The TEAC (Trolox Equivalent Antioxidant Capacity) values are expressed as Trolox equivalents, utilizing the calculated standard curve for each assay. The results are reported in μmol of Trolox equivalent *per* mL of sample ($\mu mol_{\text{Trolox equivalent}}.mL^{-1}_{\text{sample}}$).

2.11. Statistical analysis

To evaluate the effectiveness of the different conditions studied

throughout the development of this work, a one-way ANOVA (Analysis of variance) analysis was done followed by a Bonferroni post-hoc test. The results were expressed as the mean ± standard error of the mean, being statistically significant differences calculated considering an α of 95% (p-value < 0.05).

3. Results and discussion

3.1. Extraction step

3.1.1. Screening of solvents

According to the works described in the literature and as previously mentioned, organic solvents such as methanol, ethanol, or methanol/ethanol: water mixtures are conventionally applied as solvents to extract MAAs [12,20–23]. More recently, some articles were found using 100% distilled water as a way to avoid organic solvents and use greener alternatives [31–33]. From the results shown by Sun *et al.* (2021) [33], for all 4 macroalgae tested, distilled water and 25% methanol revealed similar MAAs yields of extraction. On the other hand, when comparing distilled water against 25% of ethanol, specifically for *Gracilaria* sp. (macroalgae used in the present work), 25% of ethanol demonstrated a better performance (around 32% compared to 20% of distilled water). However, the use of organic solvents and water mixtures in the extraction process implies the simultaneous extraction of hydrophilic compounds such as MAAs, non-fluorescent proteins and phycobiliproteins, and more hydrophobic compounds like chlorophylls, carotenoids, and lipids for example. Therefore, several purification steps would be required to remove all impurities. Also, porphyra-334 structure (one of the most abundant MAAs present in *Gracilaria* sp. [33]) exhibits multiple hydrophilic functional groups, promoting the creation of hydrogen bonds with adjacent water molecules [34]. Thus, and taking into account the sustainability of the process, the effect of three buffer solutions, McIlvaine (0.1 M, pH 7), PBS (1X, pH 7.4) and sodium phosphate buffer (0.1 M, pH 7) was evaluated for the extraction of MAAs and compared against distilled water, Fig. 1. Their choice was based on their pH range (needed further), preparation easiness, and because their starting materials are widely affordable and available, important issues when thinking about the process industrialization.

By analyzing Fig. 1, between the yield of extraction of distilled water and McIlvaine buffer, there are no statistically significant differences (p-value > 0.05). On the other hand, when comparing distilled water and PBS, the yield increases from 22.8 ± 0.2 to 29.6 ± 0.5 $mg_{MAAs}.g_{fresh\ biomass}^{-1}$ when PBS is the solvent (p-value < 0.05), which is even better than sodium phosphate buffer (27.3 ± 0.7 $mg_{MAAs}.g_{fresh\ biomass}^{-1}$). Therefore, PBS was the chosen solvent to proceed with the process optimization by a response surface methodology.

3.1.2. Optimization of solid–liquid extraction by a response surface methodology

After selecting the best solvent for the extraction of MAAs, a central composite rotatable design (CCRD - 2^2) was performed to optimize the process conditions. For that, two variables were studied: the extraction time (t in min, X1) and the solid–liquid ratio (SLR in $g_{MAAs}.mL_{solvent}^{-1}$, X2). A total of 11 runs were carried out with 3 central (level 0) and axial points (−1.41 and + 1.41 levels), with the MAAs yield of extraction (in $mg_{MAAs}.g_{fresh\ biomass}^{-1}$) varying from 34.9 $mg_{MAAs}.g_{fresh\ biomass}^{-1}$ in assays 2 and 4 to 56.3 $mg_{MAAs}.g_{fresh\ biomass}^{-1}$ in assay 7 (Table S1 in ESI). The predicted values were expressed by the model presented in Equation (4).

$$\text{Yield of extraction}\left(mg_{MAAs}.g_{\text{fresh biomass}}^{-1}\right) = 52.2294 + 0.3662(X1) - 0.013(X1)^2 - 28.0064(X2) + 0.5357(X1)(X2) \quad (4)$$

The Analysis of Variance (ANOVA) was used to evaluate the significance of the process variables under study and their consequent interactions, considering a 95% confidence interval with an $F_{calculated} > F_{tabulated}$ and an R^2 value of 0.735. The response surface (left side) and the respective contour plot (right side), obtained after the fitted model specified in Equation (4), are shown in Fig. 2.

As depicted in Fig. 2, and confirmed by the Pareto Chart and the predicted *vs.* observed values graph (Figs. S1 and S2 in ESI, respectively) both SLR and time of extraction variables have positive effects over the response of the predictive model (p-value < 0.05), with SLR (L) being the condition with the greatest influence (see also Table S2 in ESI). For this variable, low ratios between fresh biomass mass (g) and solvent volume (mL) greatly increase the MAAs extraction yield, in this case, the optimal condition is found at 0.0488 $g_{fresh\ biomass}.mL_{solvent}^{-1}$. Regarding the extraction time, a range of low times between 10 to 20 min is the optimal zone where an improved extraction yield is achieved. Here, from 20 min onwards, the model response is impaired, because after that point, either the solvent saturates and cannot extract more MAAs, or all MAAs content was already extracted. Thus, the optimum operating conditions were set at a SLR of 0.0488 $g_{fresh\ biomass}.mL_{solvent}^{-1}$ and 12 min of extraction time. Next, to validate the model, the extraction was repeated using the optimized conditions (n = 3). An extraction yield of 58 ± 2 $mg_{MAAs}.g_{fresh\ biomass}^{-1}$ was obtained with a relative deviation of 7.95% (Table S3 in ESI), thus validating the model.

As previously mentioned, efficient, simple, and sustainable extraction processes to recover MAAs are essential. The majority of the articles we found used extraction times exceeding 2 h, employed incubation temperatures above 45 °C, and/or involved multiple intermediate steps [12,21,22,31–33]. Apart from the energy and financial expenses associated with these methods, high temperatures prevent the preservation of temperature-sensitive compounds. Therefore, by comparison with the work developed here, ours involves only one straightforward extraction step, a short extraction time of 12 min, and operates at room temperature. Concerning extraction yield, although MAAs exhibit seasonal variations, our dry basis yield (349 ± 12 $mg_{MAAs}.g_{dry\ biomass}^{-1}$) for the same algae demonstrates comparable values to those reported by Sun

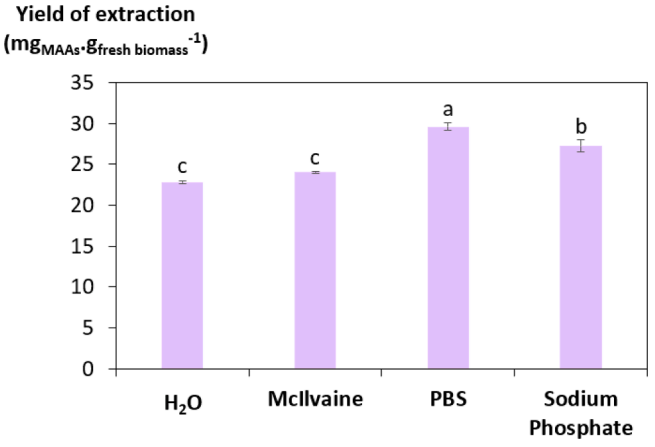

Fig. 1. MAAs yield of extraction ($mg_{MAAs}.g_{fresh\ biomass}^{-1}$) using distilled water and three buffer solutions, McIlvaine (0.1 M, pH 7), PBS (1X, pH 7.4), and sodium phosphate buffer (0.1 M, pH 7). Different lowercase letters represent statistically different values in the conditions under study (p-value < 0.05).

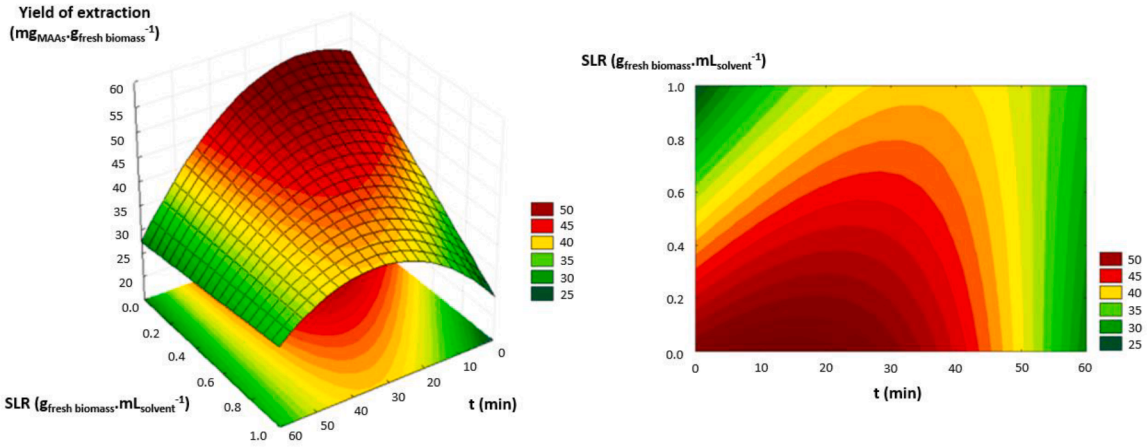

Fig. 2. Response surface plot (left side) and respective contour plot (right side) obtained for the CCRD (2^2 plus axial points), using PBS (1X, pH 7.4) as extraction solvent, regarding the independent variables: solid–liquid ratio (SLR, $g_{fresh\ biomass}.mL_{solvent}^{-1}$) and time of extraction (t, min), in terms of the dependent variable: MAAs yield of extraction (Yield of extraction, $mg_{MAAs}.g_{fresh\ biomass}^{-1}$).

et al. (2021) when utilizing a 25% ethanol extraction solvent—surpassing their outcomes achieved with distilled water [33].

3.2. High-performance liquid chromatography analysis (UHPLC-DAD-ESI/MS)

The UHPLC-DAD-ESI/MS method was used to identify the MAAs present in the obtained extract. Two compounds were identified according to the results (Fig. S3A and Table S4 of ESI). One was found in a more significant amount of 80.63%, in this case, porphyra-334, at a retention time of 1.39 min. It shows the characteristic UV–Vis spectrum and presents the pseudomolecular ion $[M-H]^-$ at m/z 345 (see Fig. S3B). The other compound, at a retention time of 1.47 min, is palythenic acid with an abundance of 5.54%. However, since the peak observed in Fig. S3C is very tiny, the *m/z* 327 ion could not be seen, which would correspond to the pseudomolecular ion $[M-H]^-$. Moreover, these findings align with the literature; porphyra-334 and palythenic acid are among the MAAs found in *Gracilaria* sp. [33]. Indeed, porphyra-334 is among the MAAs characterized by high polarity [14]. Consequently, a highly selective extraction procedure was developed by employing a highly polar solvent (PBS), facilitating the targeted extraction of porphyra-334.

3.3. Purification step

As previously mentioned, and proved by the UV–Vis spectrum of the optimized extract presented in Fig. S4 of ESI, PBS besides being the best solvent for the recovery of porphyra-334 (333 nm), other hydrophilic compounds are simultaneously extracted from *Gracilaria* sp., namely non-fluorescent proteins (at 280 nm) and phycobiliproteins (in this case, R-phycoerythrin at 565 nm). The conventional purification methods found rely on their separation by chromatography [12,20,33,35]. However, these techniques besides requiring specific and expensive equipment, are time-consuming. Therefore, more purification steps must be implemented besides the standard to achieve a pure fraction of MAAs (primary goal) and valorize the remaining compounds through a multiproduct biorefinery approach.

3.3.1. Ultrafiltration

According to the literature, porphyra-334 has a molecular weight of 346.3 Da [36], while R-phycoerythrin has around 240 kDa [37] and non-fluorescent proteins, more specifically ribulose-bisphosphate carboxylase/oxygenase (as the most abundant found [28]), approaches to 550 kDa [38]. Thus, ultrafiltration seems to be an excellent technique for this case. Furthermore, besides its simplicity, this technique has already been implemented on an industrial scale and used to purify various compounds, including phycobiliproteins [24]. Hence, two Centrifugal Filter Units of 3 kDa and 100 kDa were tested, being expected a more significant presence of non-fluorescent proteins and phycobiliproteins in the retentate and of MAAs in the permeate. Additionally, after the obtention of the retentate and 1st permeate fractions, a second ultrafiltration attempt was made by passing the 1st permeate through the same filter, obtaining a 2nd permeate fraction. This additional step was tested to verify if a more efficient separation was achieved with two consecutive ultrafiltration steps. Fig. 3 shows the compound's recovery percentage (%) in all the recovered fractions.

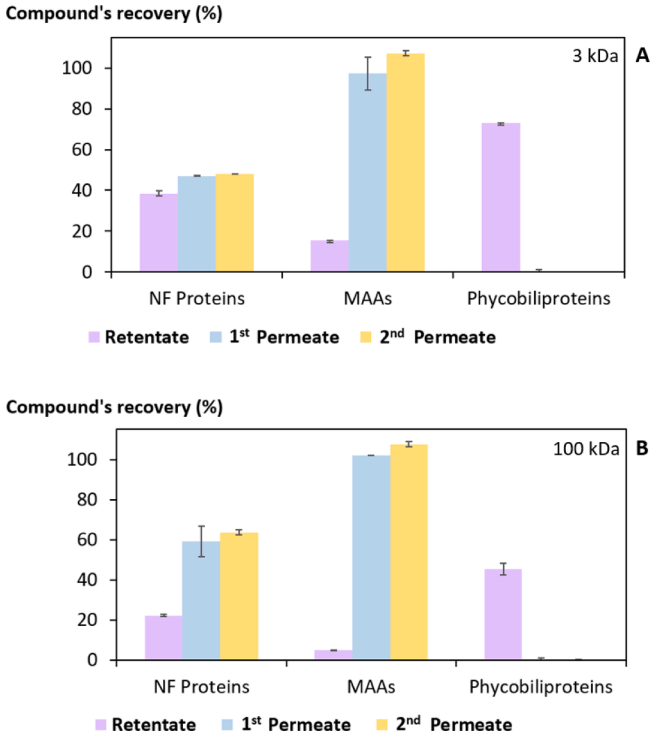

Fig. 3. Compound's recovery (NF proteins, MAAs, and phycobiliproteins) in the retentate and 1st and 2nd permeate fractions carried out considering an ultrafiltration step using two Centrifugal Filter Units of 3 kDa (A) and 100 kDa (B). NF stands for Non-Fluorescent proteins.

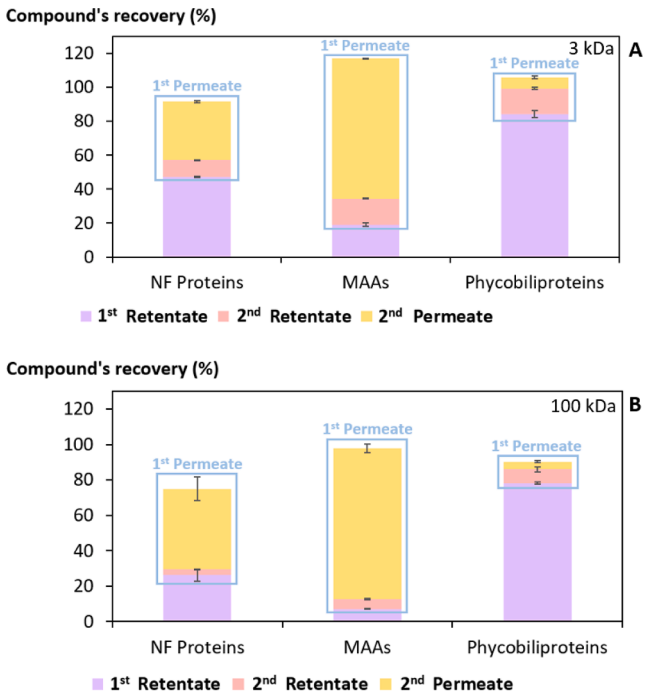

Fig. 4. Compound's recovery (NF proteins, MAAs, and phycobiliproteins) in the 1st and 2nd retentate, and 2nd permeate fractions carried out considering an ultrafiltration step using two Centrifugal Filter Units of 3 kDa (A) and 100 kDa (B). NF stands for Non-Fluorescent proteins.

From Fig. 3, it can be verified that the first ultrafiltration performed with both filter units already allowed a recovery near 100% of MAAs in the permeate fraction (1st permeate, blue bars), being 100 K the filter with the lower contamination of MAAs in the retentate fraction (retentate, purple bars), of about 5%. The results related to phycobiliproteins suggest that almost all recovery was accomplished in the retentate fraction since no UV–Vis detention of this pigment was observed in both permeate fractions (data not shown). Despite being a selective process, a possible loss of phycobiliproteins, especially in the 100 kDa filter, was seen here. Only a 45% recovery was detected, probably due to some losses to the filter (not seen in Fig. 4, see below). In the case of the non-fluorescent proteins, the expectations were not so accurate. As it can be observed, instead of being retained, in both filters a higher recovery was achieved in the permeate fraction. A possible explanation may be related to the existence of several non-fluorescent proteins of different molecular sizes in the sample. Therefore, some can pass through the filter while others are not. However, only about 20% of them are present in the retentate fraction. So, despite not being able to isolate the MAAs with this step, it was possible to isolate the phycobiliproteins with a small percentage of contamination from the other fractions. In addition, there is no need for a second ultrafiltration step at least using the same filter, as by comparing the 1st and 2nd permeate, the differences are very low.

Next, a second attempt was made, this time performing two ultrafiltration steps in a row changing for a new filter in the second ultrafiltration. The purpose of this investigation is to determine whether the lack of effectiveness in the previous second ultrafiltration was due to the use of the same filter or if a single step is already sufficient in effectively separating the compounds. This is because, by using the same filter, there is a possibility that the compounds retained during the first ultrafiltration are forming a barrier that prevents the passage of the compounds present in the second permeate. Fig. 4 presents the findings regarding this study in terms of the compound's recovery percentage (%) in all the recovered fractions.

First, comparing the results from the two filters in Fig. 4, just in terms of 1st retentate (purple bars) and 1st permeate (sum of 2nd retentate and 2nd permeate, blue rectangle), for all compounds using the 100 kDa filter a better recovery and less contamination in each fraction were observed (in accordance with Fig. 3). In other words, non-fluorescent proteins are mostly found in the permeate fraction, as well as MAAs, while phycobiliproteins were mostly found in the retentate fraction, with lower % of contamination in the other fractions compared to ultrafiltration using a 3 kDa. For phycobiliproteins (at 100 kDa), about 78% is recovered in the retentate fraction with only 12% contamination in the permeate fraction. For MAAs (at 100 kDa) about 91% are recovered in the permeate fraction with only 7% contamination in the retentate fraction. As for the non-fluorescent proteins (at 100 kDa), about 49% are recovered in the permeate fraction, while only 23% are found in the retentate fraction. For the latter, only 72% of non-fluorescent proteins in total are recovered. Possibly some losses to the filter could have happened here, since with 3 kDa the overall recovery is 91%. Regardless, 100 kDa remains the filter showing the most promising results.

Concerning the need for a second ultrafiltration, for this step to be worthwhile, a more significant retention of phycobiliproteins and almost no retention of MAAs and non-fluorescent proteins had to be observed in the 2nd retentate (pink bars). By Fig. 4, for the two filters, there is a retention of the three compounds of approximately 10–15% for 3 kDa and 3–8% for 100 kDa. As there is no significant recovery of the 3 compounds in their respective fractions of interest, there is no need to add this extra purification step to the process. Thus, after this intensive research, it can be confidently said that only a single ultrafiltration step using a 100 kDa filter unit is required to separate phycobiliproteins from non-fluorescent proteins and MAAs efficiently.

3.3.2. *Induced precipitation*

As shown so far by the results obtained here, separating MAAs from phycobiliproteins is relatively simple and easy to perform. However, to the best of our knowledge, there are no methods focused on separating MAAs from non-fluorescent proteins. Therefore, our initial efforts were based on the existing literature knowledge on protein isolation through precipitation methods. Common precipitation agents were tested, including two organic solvents (ethanol and acetone), a salt (ammonium sulfate), and a polyelectrolyte (NaPA 8000 45 wt%). The results can be found in Fig. 5.

Through Fig. 5, it is possible to notice that none of the precipitating agents were able to efficiently precipitate non-fluorescent proteins. Between the results obtained for NaPA 8000 (45 wt%) and acetone, there

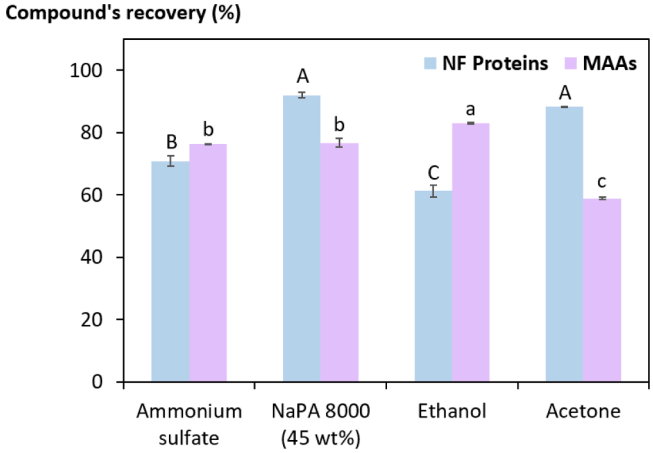

Fig. 5. Compound's recovery (NF proteins and MAAs) in the supernatant fraction after an induced precipitation with ammonium sulfate, NaPA 8000 (45 wt%), acetone and ethanol. NF stands for Non-Fluorescent proteins. Capital letters represent statistically different values in the conditions under study for NF proteins (p-value < 0.05). Lowercase letters represent statistically different values in the conditions under study for MAAs (p-value < 0.05).

are no statistically significant differences (p-value > 0.05), being only precipitated between 8–12% of proteins. Ammonium sulfate and ethanol still managed to precipitate approximately 29% and 39% of proteins (p-value < 0.05), respectively. However, this method also led to the precipitation of about 24% and 17% of MAAs (for ammonium sulfate and ethanol, respectively), indicating inefficiency. As Raj *et al.* (2021) stated, MAAs exhibit high stability because of their zwitterionic form, which is reinforced by resonance among equivalent structures, as well as the presence of hydrogen bonds [39]. Most MAAs have a hydrogen-bonded structure with over 12 bonds, which allows the occurrence of extracellular OS-MAAs (oligosaccharide-linked MAAs) already found in some cyanobacteria. These compounds feature a connection between the MAA and oligosaccharide side chains, forming strong bonds with extracellular polysaccharides and proteins [40]. Perhaps some kind of similar interaction could be taking place in this case. A link between MAAs and non-fluorescent proteins may be occurring, hence the difficulty in isolating them. An efficient separation was not attained, whether through ultrafiltration or induced precipitation with various solvents.

Some investigations have already been conducted to examine the stability of several MAAs in solutions under varying pH levels and temperatures. According to de la Coba *et al.* (2019), porphyra-334 shows stability in solutions ranging from pH 1 to 11 for up to 24 h at room temperature [13]. On the other hand, it undergoes rapid degradation when exposed to extremely high pH levels of 12 and 13. Thus, our next attempt was to carry out an induced precipitation of MAAs by changing the pH to high alkaline conditions, Fig. 6.

As shown in Fig. 6, alkaline conditions indeed caused MAAs to precipitate. Between pH 11 and 12 no statistically significant differences (p-value > 0.05) were seen, being precipitated around 40–45% of MAAs with only a small contamination of proteins, of less than 10%. The underlying reason for this phenomenon is attributed to a swift decomposition of porphyra-334, through a positive charge delocalization between the two nitrogen atoms and the connecting alkene group when exposed to basic conditions, which results in the formation of unidentified products [17].

In this sense, to obtain the highest MAAs recovery possible, an optimization of the process conditions was made. After setting the pH to 11, the time of precipitation and the concentration of NaOH (that was added to the extract to change the pH) were the variables under study for MAAs recovery, Fig. 7.

By extending the precipitation time from 24 to 72 h, there was a notable improvement in the recovery of MAAs. The recovery rate increased from less than 50% to approximately 72%, as illustrated in Fig. 7A. By increasing the NaOH concentration used, an improvement in

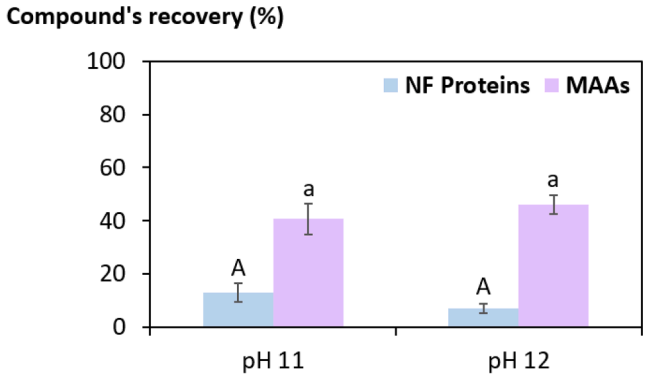

Fig. 6. Compound's recovery (NF proteins and MAAs) in the precipitate fraction after induced precipitation with pH variation, using 2 M NaOH for 24 h, at 4 °C. NF stands for Non-Fluorescent proteins. Capital letters represent statistically different values in the conditions under study for NF proteins (p-value < 0.05). Lowercase letters represent statistically different values in the conditions under study for MAAs (p-value < 0.05).

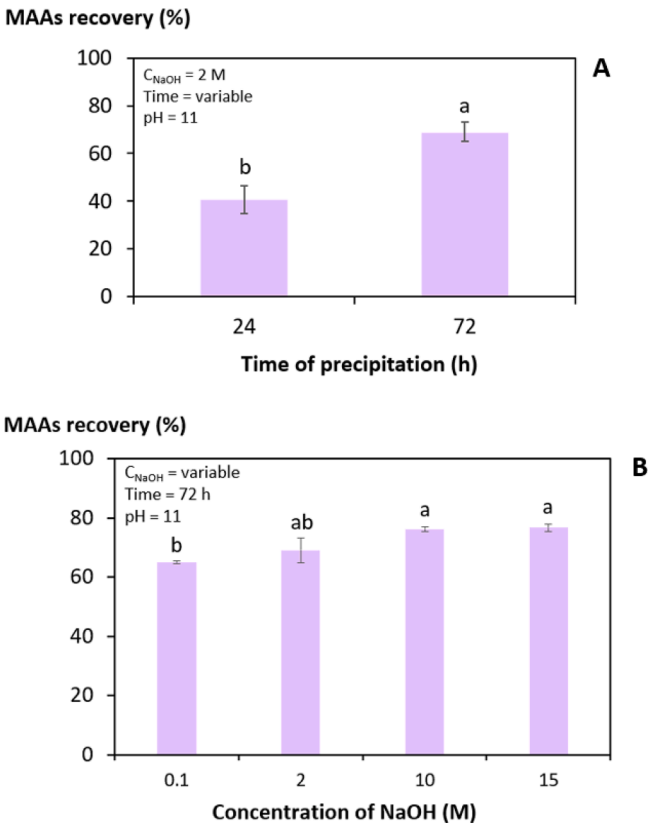

Fig. 7. MAAs recovery in the precipitate fraction after an induced precipitation considering a variation of the precipitation time (A), and a variation of NaOH concentration (B), both at pH 11. Lowercase letters represent statistically different values in the conditions under study for MAAs (p-value < 0.05).

MAAs recovery was also seen. The concentrations of 10 and 15 M were the ones with the best results, reaching a recovery of around 77%, Fig. 7B. A concentration of 10 M was selected in this case, as it yielded identical results to that of 15 M, while also helping to minimize NaOH content used. Considering that the precipitation time has a significant impact on the recovery of MAAs, it is likely that prolonging the induced precipitation beyond 72 h, if necessary for the intended application, would result in an even higher recovery rate.

3.4. Folin-Ciocalteu (total phenolic content) and ABTS scavenging assay

Exposure to ultraviolet radiation (UVR) causes oxidative stress and generates reactive oxygen species (ROS), leading to DNA damage. This oxidative DNA damage can result in mutations and hinder DNA repair processes. To mitigate these harmful effects, antioxidants play a crucial role in reducing ROS and preventing oxidative stress [41]. Certain MAAs can protect cells by absorbing UVR and dissipating the energy as heat before it reaches critical cellular targets. Additionally, these MAAs act as scavengers of free radicals, exhibiting antioxidant properties [42]. Therefore, in the present work, Folin-Ciocalteu and ABTS radical scavenging activity tests were applied to compare the total phenolic content and antioxidant activity of the initial extract (without purification) and the final extract (MAAs-rich extract obtained after purification). The results of both assays are shown in Fig. 8.

Upon examining Fig. 8, two observations can be made. Firstly, the phenolic compounds present in the initial extract were effectively separated from the final extract, resulting in a purer extract enriched with MAAs. Secondly, since the antioxidant activity is typically associated with the presence of phenolic compounds and a low abundance is observed in the final extract, the high antioxidant activity seen in Fig. 8B, can be attributed only to MAAs. Another noteworthy finding of

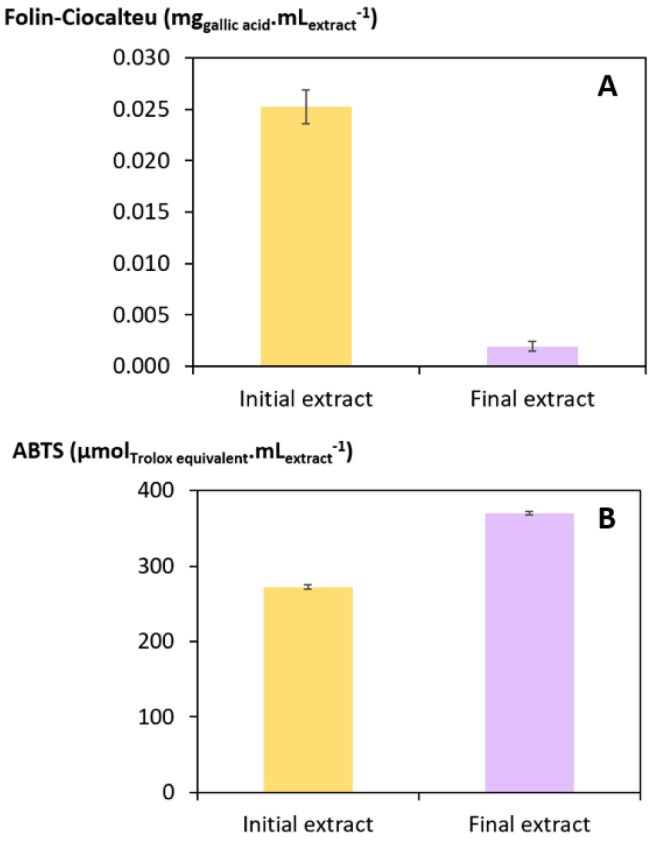

Fig. 8. Folin-Ciocalteu (Total Phenolic Content) assay expressed in $mg_{gallic\ acid}.mL_{extract}^{-1}$ (A) and ABTS scavenging assay expressed in $\mu mol_{Trolox\ equivalent}.mL_{extract}^{-1}$ (B) performed for the initial extract (without purification) and the final extract (MAAs rich extract obtained after purification).

this study is that the final extract demonstrates enhanced antioxidant activity compared to the unpurified extract (see Fig. 8B). Specifically, the initial extract exhibits an antioxidant activity value of approximately 272.2 $\mu mol_{Trolox\ equivalent}.mL_{extract}^{-1}$, whereas the purified final extract has a higher value of approximately 370.1 $\mu mol_{Trolox\ equivalent}.mL_{extract}^{-1}$, which corresponds to 69.9% and 94.7% of scavenging activity, respectively. Torres *et al.* (2018) hypothesized that the antioxidant activity of MAAs might be dependent on the pH values of the solution [42]. To test this hypothesis, they conducted an ABTS assay under different pH conditions, acidic (pH 4.6), neutral (pH 7.4), and alkaline (pH 9.6). Remarkably, both porphyra-334 and shinorine demonstrated enhanced antioxidant activity at a pH of 9.6, thereby supporting the pH-dependence hypothesis. The authors [42] argue that MAAs contain amines and carboxyl groups that can undergo ionization. Their charge state depends on the pH, with the compounds being either positively charged, neutral (zwitterionic), or negatively charged. Using MarvinSketch® software, an estimation of the isoelectric point (pI) of shinorine and porphyra-334 was found to be 3.3. When the pH surpasses their pI, the compounds acquire an increasingly negative net charge. Consequently, pH values higher than 3.3 augment the ability of these two MAAs to donate electrons, resulting in an amplified antioxidant capacity, thus providing an explanation for the pH dependency observed in the antioxidant activity of MAAs. Another recent study conducted by Nishida *et al.* (2020) further supports this hypothesis, as it demonstrated that higher pH values also lead to enhanced antioxidant scavenging activity of MAAs, particularly palythine, and porphyra-334 [31]. In the present study, the initial extract was placed in a neutral pH solution (PBS at pH 7.4), while the final extract before being resuspended in the same neutral solution underwent an induced precipitation using a highly alkaline pH of 11. This process may have been responsible for the observed increase in antioxidant activity, aligning with the underlying theory. In addition, phenolic compounds are present in the initial extract, so the increased capacity of the purified extract is even greater when both are compared, considering that its antioxidant activity derives only from MAAs.

3.5. Proposal of an integrated process for industrial implementation

Lastly, a comprehensive conceptual design of the process was formulated in Fig. 9, envisioning its industrial implementation. This design allows for the establishment of a sustainable multi-product biorefinery, where three valuable compound fractions can be recovered. The first fraction is enriched with phycoerythrin, the second fraction contains non-fluorescent proteins, and the third fraction, the primary target, comprises a high concentration of MAAs with enhanced antioxidant capacity. Overall, this approach not only maximizes the value of the macroalgae but also contributes to the development of sustainable and economically viable industrial processes.

4. Conclusions

In this study, the recovery of three purified fractions, one containing phycobiliproteins, one containing non-fluorescent proteins, and another containing MAAs, specifically porphyra-334 (main goal), was successfully accomplished. After selecting PBS as the extraction solvent, the solid–liquid ratio and the time of extraction were the variables studied through a response surface methodology to reach an optimized process with a MAAs yield of 58 ± 2 $mg_{MAAs}.g_{fresh\ biomass}^{-1}$, that corresponds to

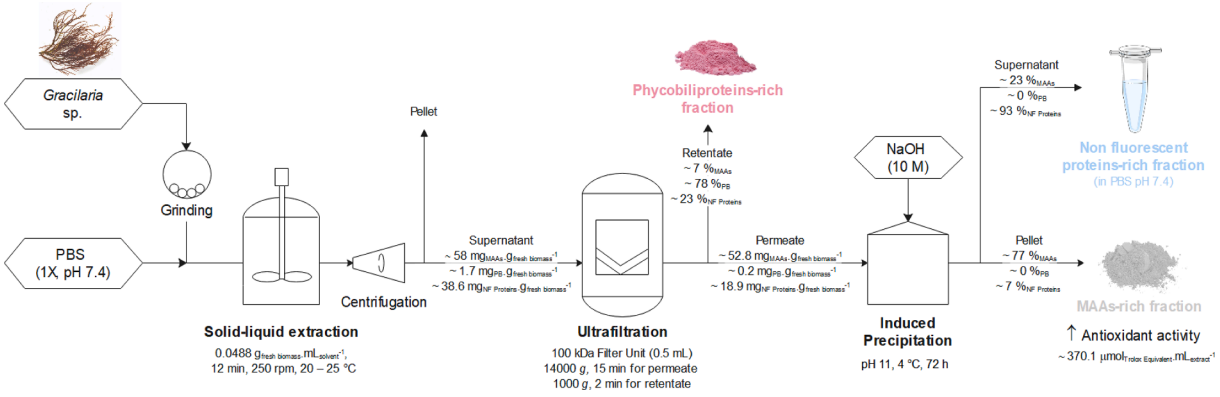

Fig. 9. Schematic representation of the final process proposed in this work including the three main steps: solid–liquid extraction using PBS (1X, pH 7.4) as extraction solvent, ultrafiltration with a 100 kDa filter unit, and induced precipitation at pH 11 for 72 h. NF stands for Non-Fluorescent proteins and PB for phycobiliproteins.

349 ± 12 $mg_{MAAs} \cdot g^{-1}_{dry\ biomass}$. For the purification step it was realized that with an ultrafiltration step, using a 100 kDa filter unit, 78% of phycobiliproteins were efficiently collected and separated from MAAs and non-fluorescent proteins. However, an additional purification step needed to be implemented to fractionate the remaining compounds. Since no method was found in literature focusing on that, several attempts were made. Lastly, it was found that an induced precipitation using a pH of 11 was able to precipitate MAAs while leaving non-fluorescent proteins in solution. After some optimization, an enriched MAAs extract with a 77% recovery and an extract enriched in non-fluorescent proteins with a recovery of 93% were obtained. Next, the hypothesis that MAAs antioxidant activity is pH dependent and that the high antioxidant capacity of the purified MAAs extract was only attributed to MAAs was proved. Consequently, an enhanced MAAs pure extract was successfully obtained, making it suitable for incorporation into cosmetic formulations. Lastly, this work also encompasses a proposed integrated process for industrial implementation of the process here developed. Aiming not only to contribute to the advancement of a marine bio-based economy, but also to the utilization of natural resources in an environmentally responsible manner.

Declaration of competing interest

The authors declare that they have no known competing financial interests or personal relationships that could have appeared to influence the work reported in this paper.

Acknowledgements

This work was developed within the scope of the project CICECO-Aveiro Institute of Materials, UIDB/50011/2020 (DOI 10.54499/UIDB/50011/2020), UIDP/50011/2020 (DOI 10.54499/UIDP/50011/2020) & LA/P/0006/2020 (DOI 10.54499/LA/P/0006/2020), financed by national funds through the FCT/MCTES (PIDDAC). This work was co-financed by the FCT project with the Ref: 2022.04670.PTDC. The authors would like to thank "Fundação de Amparo à Pesquisa do Estado de São Paulo – FAPESP" for the fellowship of L.S. Contieri (2020/03623-2) and L.M. de Souza Mesquita (2020/08421-9), and FCT for the doctoral grant of B.M.C Vaz (2022.13816.BD).

Appendix A. Supplementary data

Supplementary data to this article can be found online at https://doi.org/10.1016/j.seppur.2025.132200.

Data availability

Data will be made available on request.

References

[1] A. Merino-Saum, M.G. Baldi, I. Gunderson, B. Oberle, Articulating natural resources and sustainable development goals through green economy indicators: a systematic analysis, Resour. Conserv. Recycl. 139 (2018) 90–103, https://doi.org/10.1016/j.resconrec.2018.07.007.
[2] A. Lampert, Over-exploitation of natural resources is followed by inevitable declines in economic growth and discount rate, Nat. Commun. 10 (2019) 1419, https://doi.org/10.1038/s41467-019-09246-2.
[3] P. Kumar, Innovative tools and new metrics for inclusive green economy, Curr. Opin. Environ. Sustain. 24 (2017) 47–51, https://doi.org/10.1016/j.cosust.2017.01.012.
[4] L'Oréal, L'Oréal for the Future, 2020. https://www.loreal.com/-/media/project/loreal/brand-sites/corp/master/lcorp/documents-media/publications/l4f/loreal-for-the-future–booklet.pdf?rev=265bdbc0ded24a95b3aae0aba278b8bd&hash=81C863AF659C16D7C5550B0F4976B910.
[5] A.K. Koyande, P.-L. Show, R. Guo, B. Tang, C. Ogino, J.-S. Chang, Bio-processing of algal bio-refinery: a review on current advances and future perspectives, Bioengineered. 10 (2019) 574–592, https://doi.org/10.1080/21655979.2019.1679697.
[6] K.W. Chew, J.Y. Yap, P.L. Show, N.H. Suan, J.C. Juan, T.C. Ling, D.-J. Lee, J.-S. Chang, Microalgae biorefinery: high value products perspectives, Bioresour. Technol. 229 (2017) 53–62, https://doi.org/10.1016/j.biortech.2017.01.006.
[7] M. Bhattacharya, S. Goswami, Microalgae – A green multi-product biorefinery for future industrial prospects, Biocatal. Agric. Biotechnol. 25 (2020) 101580, https://doi.org/10.1016/j.bcab.2020.101580.
[8] E.S. Okeke, O. Ejeromedoghene, C.O. Okoye, T.P.C. Ezeorba, R. Nyaruaba, C. K. Ikechukwu, A. Oladipo, J.I. Orege, Microalgae biorefinery: an integrated route for the sustainable production of high-value-added products, Energy Convers. Manag. X 16 (2022) 100323, https://doi.org/10.1016/j.ecmx.2022.100323.
[9] L.M.L. Laurens, J. Markham, D.W. Templeton, E.D. Christensen, S. Van Wychen, E. W. Vadelius, M. Chen-Glasser, T. Dong, R. Davis, P.T. Pienkos, Development of algae biorefinery concepts for biofuels and bioproducts; a perspective on process-compatible products and their impact on cost-reduction, Energ. Environ. Sci. 10 (2017) 1716, https://doi.org/10.1039/c7ee01306j.
[10] M. Álvarez-Viñas, N. Flórez-Fernández, M.D. Torres, H. Domínguez, Successful approaches for a red seaweed biorefinery, Mar. Drugs 17 (2019) 620, https://doi.org/10.3390/md17110620.
[11] R.P. Rastogi, A. Incharoensakdi, Analysis of UV-absorbing photoprotectant mycosporine-like amino acid (MAA) in the cyanobacterium Arthrospira sp. CU2556, Photochem. Photobiol. Sci. 13 (2014) 1016–1024, https://doi.org/10.1039/c4 pp00013g.
[12] F. de la Coba, J. Aguilera, F.L. Figueroa, M.V. de Gálvez, E. Herrera, Antioxidant activity of mycosporine-like amino acids isolated from three red macroalgae and one marine lichen, J. Appl. Phycol. 21 (2009) 161–169, https://doi.org/10.1007/s10811-008-9345-1.
[13] F. de la Coba, J. Aguilera, N. Korbee, M.V. de Gálvez, E. Herrera-Ceballos, F. Álvarez-Gómez, F.L. Figueroa, UVA and UVB photoprotective capabilities of topical formulations containing mycosporine-like amino acids (MAAs) through different biological effective protection factors (BEPFs), Mar. Drugs 17 (2019) 55, https://doi.org/10.3390/md17010055.
[14] J. Vega, G. Schneider, B.R. Moreira, C. Herrera, J. Bonomi-Barufi, F.L. Figueroa, Mycosporine-like amino acids from red macroalgae: UV-photoprotectors with potential cosmeceutical applications, Appl. Sci. 11 (2021) 5112, https://doi.org/10.3390/app11115112.
[15] S. Fonseca, M.N. Amaral, C.P. Reis, L. Custódio, Marine natural products as innovative cosmetic ingredients, Mar. Drugs 21 (2023) 170, https://doi.org/10.3390/md21030170.
[16] M. Singh, E. Sharma, Novel and secure trend for photo protection - a hallmark of plant metabolites as UV filters, Int. J. Recent Sci. Res. 5 (2014) 322–325. http://recentscientific.com/sites/default/files/Download_858.pdf.
[17] R. Losantos, D. Sampedro, M.S. Churio, Photochemistry and photophysics of mycosporine-like amino acids and gadusols, nature's ultraviolet screens, Pure Appl. Chem. 87 (2015) 979–996, https://doi.org/10.1515/pac-2015-0304.
[18] F.L. Figueroa, Mycosporine-like amino acids from marine resource, Mar. Drugs 19 (2021) 18, https://doi.org/10.3390/MD19010018.
[19] T. Tsunoda, T. Mahmud, Aminocyclitols, in: H.-W. (Ben) Liu, T.P. Begley (Eds.), Compr. Nat. Prod. III, 3rd editio, Elsevier, 2020: pp. 553–587. https://doi.org/10.1016/b978-0-12-409547-2.14708-0.
[20] A. Torres, C.D. Enk, M. Hochberg, M. Srebnik, Porphyra-334, a potential natural source for UVA protective sunscreens, Photochem. Photobiol. Sci. 5 (2006) 432–435, https://doi.org/10.1039/b517330m.
[21] R.P. Sinha, M. Klisch, A. Groniger, D.-P. Hader, Mycosporine-like amino acids in the marine red alga *Gracilaria cornea* — effects of UV and heat, Environ. Exp. Bot. 43 (2000) 33–43, https://doi.org/10.1016/S0098-8472(99)00043-X.
[22] K. Whitehead, J.I. Hedges, Analysis of mycosporine-like amino acids in plankton by liquid chromatography electrospray ionization mass spectrometry, Mar. Chem. 80 (2002) 27–39, https://doi.org/10.1016/S0304-4203(02)00096-8.
[23] N.N. Rosic, C. Braun, D. Kvaskoff, Extraction and Analysis of Mycosporine-Like Amino Acids in Marine Algae, in: D.B. Stengel, S. Connan (Eds.), Nat. Prod. From Mar. Algae, Springer Science+Business Media New York, 2015: pp. 119–129. https://doi.org/10.1007/978-1-4939-2684-8_6.
[24] M. Martins, B.P. Soares, J.H.P.M. Santos, P. Bharmoria, M.A. Torres Acosta, A.C.R. V. Dias, J.A.P. Coutinho, S.P.M. Ventura, Sustainable strategy based on induced precipitation for the purification of phycobiliproteins, ACS Sustain. Chem. Eng. 9 (2021) 3942–3954, https://doi.org/10.1021/acssuschemeng.0c09218.
[25] A. Dean, D. Voss, Design and Analysis of Experiments, 1st edn, Springer, New York, 1999. https://doi.org/10.1007/b97673.
[26] M.I. Rodrigues, A.F. Lemma, Planejamento de Experimentos e Otimização de Processos, 3rd ed., Casa do Pão Editora, 2014.
[27] T. Scientific, Acetone precipitation of proteins, TECH TIP # 49 Acetone. TR0049.1 (2009) 1–2.
[28] F.A. Vicente, I.S. Cardoso, M. Martins, C.V.M. Gonçalves, A.C.R.V. Dias, P. Domingues, J.A.P. Coutinho, S.P.M. Ventura, R-phycoerythrin extraction and purification from fresh *Gracilaria* sp. using thermo-responsive systems, Green Chem. 21 (2019) 3816–3826, https://doi.org/10.1039/C9GC00104B.
[29] E.R. Coscueta, L.P. Malpiedi, B.B. Nerli, Micellar systems of aliphatic alcohol ethoxylates as a sustainable alternative to extract soybean isoflavones, Food Chem. 264 (2018) 135–141, https://doi.org/10.1016/j.foodchem.2018.05.015.
[30] B. Gonçalves, V. Falco, J. Moutinho-Pereira, E. Bacelar, F. Peixoto, C. Correia, Effects of elevated CO2 on grapevine (*Vitis vinifera* L.): volatile composition, phenolic content, and in vitro antioxidant activity of red wine, J. Agric. Food Chem. 57 (2009) 265–273, https://doi.org/10.1021/jf8020199.
[31] Y. Nishida, Y. Kumagai, S. Michiba, H. Yasui, H. Kishimura, Efficient extraction and antioxidant capacity of mycosporine-like amino acids from Red Alga Dulse

Palmaria palmata in Japan, Mar. Drugs 18 (2020) 502, https://doi.org/10.3390/md18100502.
[32] P. Chaves-Peña, F. de la Coba, F.L. Figueroa, N. Korbee, Quantitative and qualitative HPLC analysis of mycosporine-like amino acids extracted in distilled water for cosmetical uses in four Rhodophyta, Mar. Drugs 18 (2020) 27, https://doi.org/10.3390/md18010027.
[33] Y. Sun, X. Han, Z. Hu, T. Cheng, Q. Tang, H. Wang, X. Deng, X. Han, Extraction, isolation and characterization of mycosporine-like amino acids from four species of red macroalgae, Mar. Drugs 19 (2021) 615, https://doi.org/10.3390/md19110615.
[34] Y. Harada, M. Hatakeyama, S. Maeda, Q. Gao, K. Koizumi, Y. Sakamoto, Y. Ono, S. Nakamura, Molecular design learned from the natural product Porphyra-334: molecular generation via chemical variational autoencoder versus database mining via similarity search, a comparative study, ACS Omega. 7 (2022) 8581–8590, https://doi.org/10.1021/acsomega.1c06453.
[35] J. Vega, D. Bárcenas-Pérez, D. Fuentes-Ríos, J.M. López-Romero, P. Hrouzek, F. L. Figueroa, J. Cheel, Isolation of mycosporine- like amino acids from red macroalgae and a marine lichen by high-performance countercurrent chromatography: A strategy to obtain biological UV-filters, Mar. Drugs 21 (2023) 357, https://doi.org/10.3390/md21060357.
[36] Royal Society of Chemistry, ChemSpider, (2023). https://www.chemspider.com/Chemical-Structure.29390215.html (accessed June 2, 2023).
[37] A.V. Klotz, A.N. Glazer, Characterization of the Bilin Attachment Sites in R-Phycoerythrin*, J. Biol. Chem. 260 (1985) 4856–4863, https://doi.org/10.1016/S0021-9258(18)89150-5.
[38] G.D. Heda, M.T. Madigan, Purification and characterization of the thermostable ribulose-1,5-bisphosphate carboxylase/oxygenase from the thermophilic purple bacterium *Chromatiurn tepidum*, Eur. J. Biochem. 184 (1989) 313–319, https://doi.org/10.1111/j.1432-1033.1989.tb15021.x.
[39] S. Raj, A.M. Kuniyil, A. Sreenikethanam, P. Gugulothu, R.B. Jeyakumar, A. K. Bajhaiya, Microalgae as a source of mycosporine-like amino acids (MAAs); advances and future prospects, Int. J. Environ. Res. Public Health 18 (2021) 12402, https://doi.org/10.3390/ijerph182312402.
[40] L. Ferroni, M. Klisch, S. Pancaldi, D.P. Häder, Complementary UV-absorption of mycosporine-like amino acids and scytonemin is responsible for the UV-insensitivity of photosynthesis in *Nostoc flagelliforme*, Mar. Drugs 8 (2010) 106–121, https://doi.org/10.3390/md8010106.
[41] V. Geraldes, E. Pinto, Mycosporine-like amino acids (MAAs): biology, chemistry and identification features, Pharmaceuticals. 14 (2021) 63, https://doi.org/10.3390/ph14010063.
[42] P. Torres, J. Pires Santos, F. Chow, M.J. Pena Ferreira, D.Y.A.C. dos Santos, Comparative analysis of *in vitro* antioxidant capacities of mycosporine-like amino acids (MAAs), Algal Res. 34 (2018) 57–67, https://doi.org/10.1016/j.algal.2018.07.007.